J Mater Sci (2007) 42:5074–5079
DOI 10.1007/s10853-006-0479-8

Effects of post-deposition chemical treatment on the formation of mesoporous titania films

Nobuaki Kitazawa · Hirokazu Sato · Yoshihisa Watanabe

Received: 5 December 2005 / Accepted: 31 May 2006 / Published online: 22 February 2007

Abstract Mesoporous titania films have been synthesized by a modified sol–gel method in conjunction with amphiphilic triblock copolymers. The effects of ammonia vapor treatment on the formation of mesoporous structures were investigated. Mesoporous titania films with hexagonal structures were obtained by ammonia vapor treatment. Without ammonia vapor treatment, it was found that the mesoporous structures collapse due to crystallization. The framework of mesoporous titania was found to be amorphous. Mesoporous titania films prepared by ammonia vapor treatment showed thermal stability up to 500 °C. Mesoporous samples showed better photo-catalytic activity than anatase titania films under UV-light irradiation.

Introduction

Ever since the discovery of mesoporous silicates by researchers at Mobil Oil Corporation [1, 2], there has been great interest in the synthesis and application of mesoporous oxide materials [3, 4]. In work to date, mesoporous powders of various oxides have been prepared based on the use of sol–gel chemistry in conjunction with surfactants [5–8]. From the scientific point of view, the reliable processing of mesoporous oxides into thin films has attracted considerable interest. Recently, mesoporous silica films have been prepared by the evaporation-induced self-assembly (EISA) of surfactants [9–12]. The EISA process has been extended to mesoporous transition metal oxides [13–15]. Among them, mesoporous titania (TiO_2) is an attractive material due to its high photo-catalytic activity under UV light irradiation.

Since the first pioneering work by Honda and Fujishima [16], a great deal of research has been conducted in order to improve the photo-catalytic activity of titania by enhancing its textural and morphological characteristics [13, 17, 18]. The high specific surface area provided by mesoporous titania should offer enhanced photo-catalytic activity. As a general synthetic approach for the preparation of mesoporous oxides, amphiphilic block copolymers have emerged as structure-directing agents [11, 19, 20]. To our knowledge, the synthesis of mesoporous titania is more complicated when compared with that of mesoporous silica [21–23]. In most cases, mesoporous structures collapse during heat-treatment. More recently, highly ordered mesoporous titania films have been prepared and characterized [24–26]. Carefully controlled synthesis conditions enable the fabrication of mesoporous titania films.

Generally, most titanium alkoxides are highly reactive toward hydrolysis and condensation, leading to the formation of uncontrollable precipitates [27]. Chemical modification using acetates, amines and β-diketones has been employed for the stabilization of titanium alkoxides [28, 29]. However, the chemical reactivity of modified titanium alkoxides is strongly reduced vis-a-vis hydrolysis and condensation. On the contrary, it is interesting to note that clear and stable titanium alkoxide solutions can be obtained without chemical

N. Kitazawa (✉) · H. Sato · Y. Watanabe
Department of Materials Science and Engineering, National Defense Academy, 1-10-20 Hashirimizu, Yokosuka, Kanagawa 239-8686, Japan
e-mail: nkita@nda.ac.jp

modification in the presence of a large amount of acid [27]. Acid behaves as a condensation inhibitor. As-synthesized films prepared from precursor solutions at high pH, therefore, probably possess a fragile titania framework. It is well known that ammonia can act as a condensation promoter [27]. Therefore, stabilization of the titania framework can be expected when as-synthesized films are treated by ammonia vapor.

In this study, mesostructured titania films have been synthesized by modifying the sol–gel method in conjunction with amphiphilic triblock copolymers under acidic conditions. The effect of ammonia vapor treatment on the formation of mesoporous titania films has also been investigated.

Experimental procedure

Reagent grade titanium (IV) butoxide [$Ti(O–nC_4H_9)_4$, abbreviated as TBOT hereafter, Aldrich], ethyl alcohol (C_2H_5OH, 99.5 %, Wako Chemical), hydrochloric acid (35.5 wt% HCl-aq, Wako Chemical) and distilled water were used as raw materials. As a structure-directing agent, Pluronic P123 with a poly(ethylene oxide)-poly(propylene oxide)-poly(ethylene oxide) sequence ($EO_{20}PO_{70}EO_{20}$, average molecular weight = 5,800, BASF) was used as received without further purification.

In a typical preparation, TBOT (1.70 g) was dissolved in a mixture of HCl-aq (0.38 g) and C_2H_5OH (4.60 g) under vigorous stirring (about 1000 rpm) in air at room temperature. After 90 min of stirring, distilled water (120 μl) and then Pluronic P123 (0.51 g) were added directly to the TBOT/HCl/C_2H_5OH mixture. Distilled water was added using a micro pipette (Nichipet EX, Nichiro). A glass tube (30 ml in volume) with a Teflon cap was used as the vessel. The mixture was aged at room temperature for 24 h under stirring at 400 rpm in air. The favorable TBOT:C_2H_5OH:HCl:H_2O:Pluronic P123 molar composition was found to be $1:20:0.75:4:1.76 \times 10^{-2}$. After a homogeneous sol was obtained, wet-gel films were deposited on silica glass and Si (100) substrates ($20 \times 20 \times 0.5$ mm^3 in size) by spin-coating at 2500 rpm for 1 min. Spin-coating was carried out in a humidity controlled (less than 30%RH) dry box in air.

As-deposited samples were dried for 24 h in an ordinary air atmosphere (25 °C, 60%RH). After drying, a sample was loaded vertically using a clip into a polypropylene vessel (28 mm$\phi \times 110$ mm, 50 ml in volume). Subsequently, 20 μl of aqueous ammonia was added in the vessel by using a micro pipette (Nichipet EX, Nichiro). The vessel was then sealed with a Teflon cap. The pH value of aqueous ammonia was varied from 10.8 to 12.0. The sealed polypropylene vessel, with a sample and aqueous ammonia, was loaded in an oven. Ammonia vapor treatment was carried out in the oven at 60 °C for 24 h. Samples, with and without ammonia vapor treatment, were calcined for 4 h in air at several temperatures over the range of 200–700 °C. The film thickness of calcined samples varied from 1200 to 1500 nm.

X-ray diffraction (XRD) experiments were performed using a X-ray diffractometer (Rigaku RINT-2000) with CrKα radiation (20 kV, 30 mA). Transmission electron microscopy (TEM) and selected area electron diffraction (SAED) images were recorded using an electron microscope (Hitachi HF-2000) operated at 200 kV. Samples were detached from their Si substrates and dispersed in ethyl alcohol (C_2H_5OH, 99.5%, Wako Chemical). Thin sample fragments of samples were collected on holey carbon films on copper grids (Type A grid, Okenshoji).

Photo-catalytic activity of samples was evaluated by measuring the decomposition rate of Methylene Blue ($C_{16}H_{18}N_3S \cdot Cl \cdot 2H_2O$, Wako Chemical) under UV-light irradiation. Samples on Si substrates were cut ($9 \times 20 \times 0.5$ mm^3) and then immersed in 4.0 ml of an aqueous Methylene Blue solution (1×10^{-5} mol/l). A vitreous quartz cell ($10 \times 10 \times 50$ mm^3) was used as a vessel. UV-light irradiation was carried out using a 400 W high-pressure mercury lamp with a band-pass filter (U-340, Sigma Koki). A water-filled cell was also used as an infrared filter. The decomposition rate of Methylene Blue solution was recorded at different time intervals using a UV–Vis spectrophotometer (JASCO V-570 Spectrophotometer).

Results and discussions

Figure 1 shows the results of XRD measurements for (a) as-deposited and (b) calcined samples. The as-deposited sample showed an intense and narrow Bragg reflection at 1.49° and a much weaker one at 2.85°. These peaks are indexed as the (100) and (200) reflections, respectively, of a hexagonal mesostructure. This result can be explained by the preferential arrangement of micellar cylinders parallel to the substrate surface. In contrast, the calcined sample showed diffuse scatterings in the 2θ range of 1–4°, suggesting that the heat-treatment collapsed the hexagonal mesostructure.

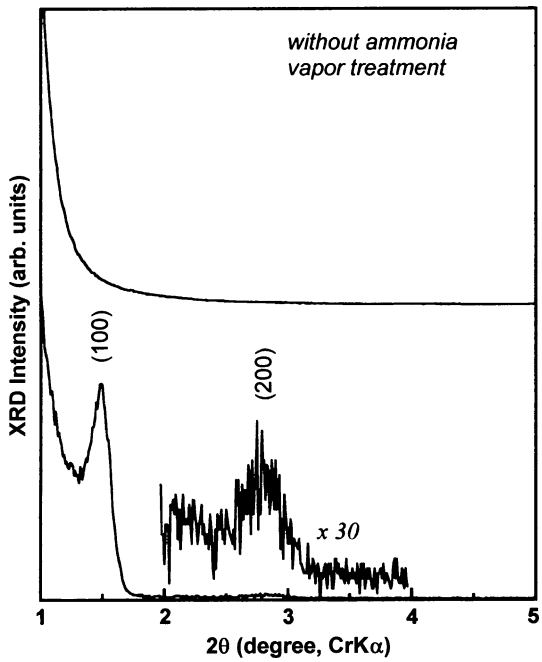

Fig. 1 XRD patterns of (**a**) as-deposited and (**b**) calcined samples prepared from a precursor solution with a P123/TBOT molar ratio of $1{:}1.76 \times 10^{-2}$. Note that the calcined sample was heat-treated at 400 °C for 4 h

Figure 2 shows the TEM pictures of the samples calcined at (a) 300 °C and (b) 400 °C for 4 h. SAED patterns are also shown in the Figure. Bright sections indicate the pores while dark parts represent titania matrices. Nanometer-sized (less than 10 nm) particles were observed when the sample was calcined at 300 °C.

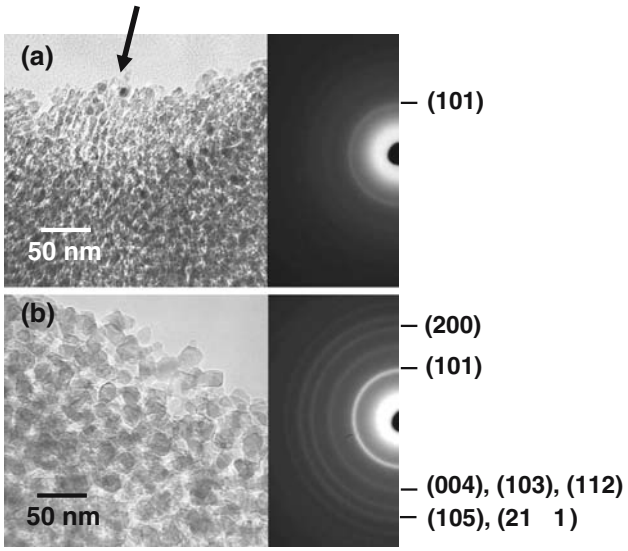

Fig. 2 TEM image of samples calcined at (**a**) 300 °C and (**b**) 400 °C for 4 h. Corresponding SAED patterns are also shown in the figure

It is interesting to note that the degraded hexagonal structures were observed. As indicated by an arrow in the picture, pores and particles seem to be regularly arranged near the edge. The SAED pattern of the sample showed the weak (101) reflection of anatase titania. Nano-crystalline titania precipitates with a well-defined SAED pattern were observed for the sample calcined at 400 °C. These diffraction rings were indexed as the (101), (004), (103), (112), (200), (105) and (211) reflections of anatase titania [30]. The sample also showed disordered structures with intergranular pores. From these results, calcination-induced crystallization was one of the possible reasons for the degradation.

Figure 3 shows XRD patterns of samples after ammonia vapor treatment (dotted lines) and after subsequent calcinations at 400 °C for 4 h (solid lines). Initial pH values of aqueous ammonia solutions were (a) 11.2, (b) 11.4 and (c) 11.6, respectively. As

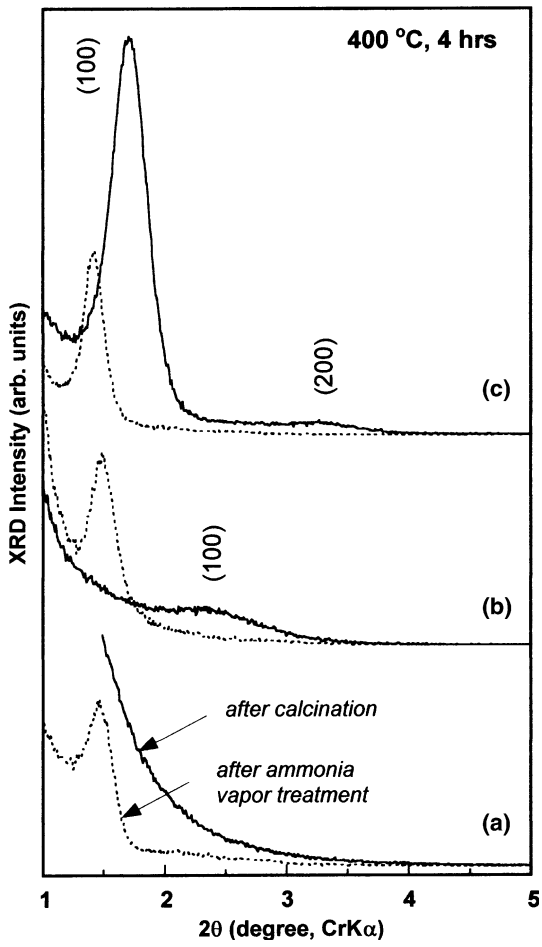

Fig. 3 XRD patterns of samples after ammonia vapor treatment (dotted lines) and calcined samples heat-treated at 400 °C for 4 h. (solid lines). The initial pH values of aqueous ammonia are (**a**) 11.2, (**b**) 11.4 and (**c**) 11.6, respectively

indicated by dotted lines, samples after ammonia vapor treatment showed the (100) reflection of hexagonal structures. After calcination, no diffraction peaks were observed for sample (a). The weak and broad (100) reflection was observed for sample (b). Sample (c) exhibited an intense and narrow Bragg reflection at 1.70° and a weaker one at 3.35°, respectively. These peaks can be indexed respectively as the (100) and (200) reflections of a hexagonal structure with a unit cell parameter of $a = 7.8 \pm 0.2$ nm. Therefore, one can surmise that ammonia vapor treatment affects the formation of mesoporous titania. It should be noted that samples became detached after calcination when the initial pH value of aqueous ammonia was more than 12.0.

Figure 4 shows the results of TEM observation for calcined samples prepared by ammonia vapor treatment. The pH values of aqueous ammonia solutions were (a) 11.2, (b) 11.4 and (c) 11.6, respectively. SAED patterns are also shown in the Figure. In picture (a), the sample consisted of nanocrystalline titana particles. The average grain size of titania particles was estimated to be about 10 nm. A well-defined SAED pattern corresponding to the anatase phase was also observed. A continuous titania framework with disordered mesopores was observed for sample (b). In picture (c), the sample exhibited well-ordered mesoporous structures. The right side of the image shows a hexagonal structure and left side represents a cellular-like structure. The titania wall thickness was estimated to be about 2.0 nm. However, the wall of titania appeared to be amorphous.

Figure 5 shows TEM pictures of mesoporous samples calcined at (a) 500 °C, (b) 600 °C and (c) 700 °C, respectively. The pH value of aqueous ammonia was 11.6. In picture (a), the sample showed an ordered hexagonal structure but the titania matrices appeared to be amorphous. In picture (b), nanocrystalline titania particles with degraded hexagonal structures were observed. In picture (c), nanocrystalline titania particles with disordered structures were observed. The (101), (004), (103), (112), (200), (105) and (211) reflections of the anatase phase were clearly observed for the sample. The results of TEM observations for the calcined samples showed good agreement with XRD results. Samples showed clear (100) and (200)

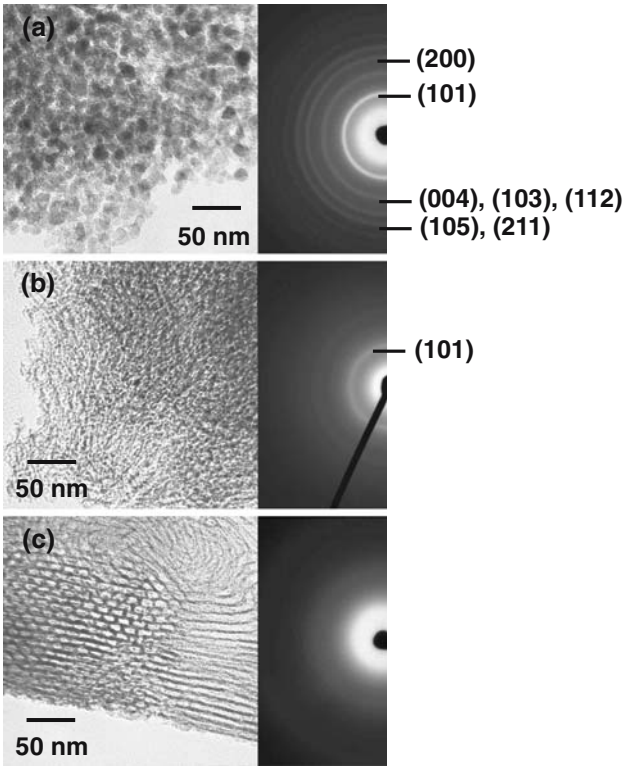

Fig. 4 TEM pictures of calcined samples after ammonia vapor treatment. The initial pH values of aqueous ammonia are (**a**) 11.2, (**b**) 11.4 and (**c**) 11.6, respectively. Corresponding SAED patterns are also shown. Note that the samples were calcined at 400 °C for 4 h

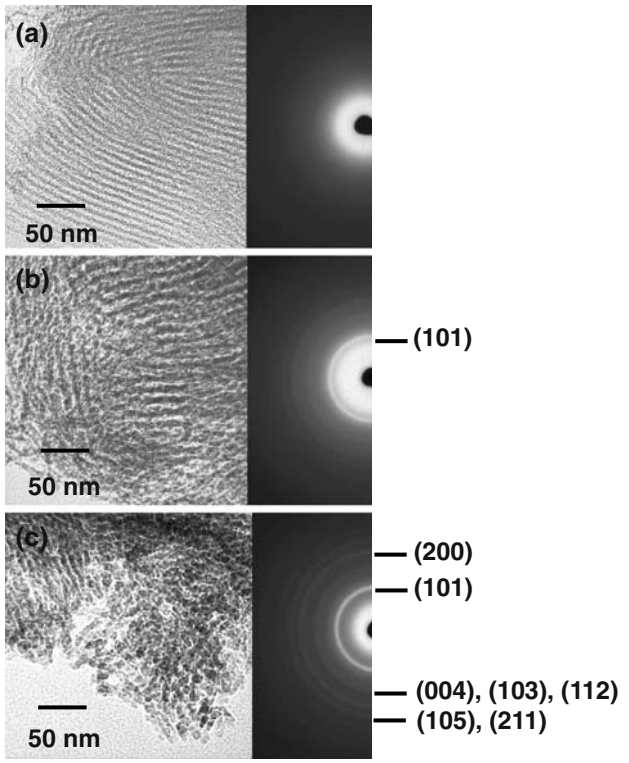

Fig. 5 TEM pictures of mesoporous samples calcined at (**a**) 500 °C, (**b**) 600 °C and (**c**) 700 °C for 4 h. The initial pH value of aqueous ammonia solution was 11.6. Corresponding SAED patterns of each sample are also shown

reflections of hexagonal structures up to 500 °C. At above 600 °C, the (100) peak decreased and shifted towards larger 2θ values. This can be explained by the degradation of the mesoporous structure during crystallization. A further decrease in the peak intensity occurred at 700 °C. Therefore, mesoporous titania prepared by ammonia vapor treatment showed thermal stability only up to 500 °C.

Figure 6 shows changes in the relative absorption intensity as a function of irradiation time. The decomposition rate of Methylene Blue was estimated from the relative absorption intensity (I_t/I_0) as a function of irradiation time. I_0 means the absorption coefficient of aqueous Methylene Blue before irradiation and I_t represents that of irradiated for t min. The absorption coefficient was estimated at 665 nm. As shown in curve (a), I_t/I_0 values decreased very slightly when aqueous Bethylene Blue was irradiated without titania films. In curve (b), the sample showed clear photo-catalytic activity. The I_t/I_0 decreased to about 80% after irradiation for 150 min. Marked differences were observed for samples with mesoporous structures. As shown in curve (c), the decomposition rate increased about two times compared with that of the nanocrystalline titana film. Further improvement was observed for sample (d). The I_t/I_0 decreased to about 35% after irradiation for 150 min. According to the SAED pattern, amorphous mesoporous titania films showed better photocatalytic activity than nano-crystalline titalia films. No further improvement was observed for the sample calcined at 600 °C, as shown in curve (e).

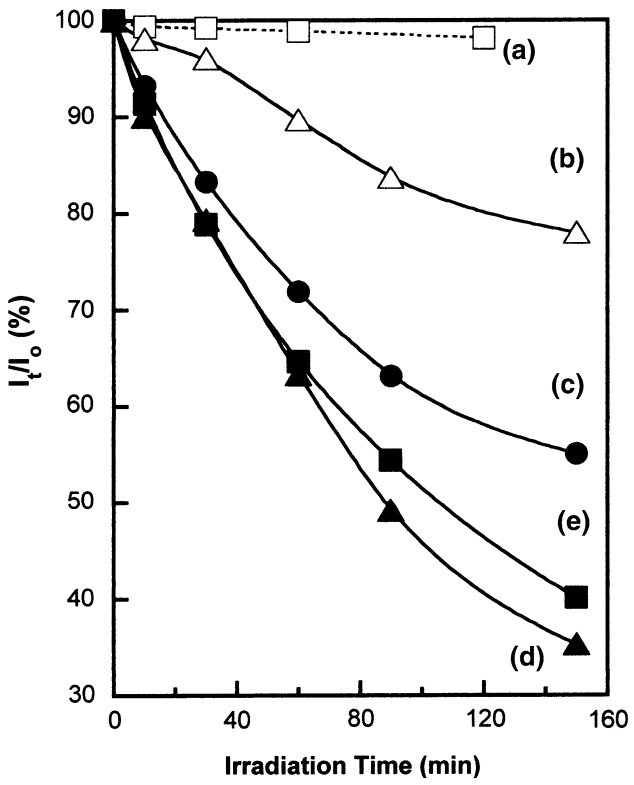

Fig. 6. Changes in the relative absorption intensity as a function of irradiation time: (**a**) without titania films, (**b**) nanocrystalline titania films and mesoporous titania samples calcined at (**c**) 400 °C, (**d**) 500 °C and (**e**) 600 °C for 4 h, respectively

It is generally accepted that anatase titania exhibits better photo-catalytic activity than amorphous and rutile titania [17]. This study clarifies how mesoporous structures affected photo-catalytic activity. As shown in Fig. 6, amorphous mesoporous titania films showed better photo-catalytic activity than anatase nanocrystalline titania films. Therefore, the mesoporous structures were a very important factor in the enhanced photo-catalytic activity. Mesoporous samples showed hexagonal structures, they exhibited enhanced photo-catalytic activity. This result suggested that a part of the mesopores act as open channels. The formation of a continuous 3D mesoporous structure is very attractive for practical applications. In the synthesis of mesoporous silica films, the EO/PO ratio affects the formation of mesostructure [10, 33]. Mesoporous silica films with a continuous 3D mesoporous structure have been synthesized using PEO-PPO-PEO block copolymers with higher EO/PO ratios above 1.5, e.g. Pluronic F127 for example [10]. Owing to its complexity of the procedure, it is difficult to fully understand the specific mechanism during sol–gel thin film deposition and ammonia vapor treatment, since there are many synthetic parameters which affect the formation of mesoporous structure. Therefore, suitable controls of synthesis conditions could allow the preparation of mesoporous titania films with continuous 3D pores and improved activity. It is believed that ammonia vapor treatment will be one of the indispensable processes for the preparation of mesoporous titania films.

Conclusion

In this study, the effect of ammonia vapor treatment on the formation of mesoporous titania films has been investigated. Without ammonia vapor treatment, calcination-induced degradation of mesostructures occurred due to crystallization. Mesoporous titania films have been successfully fabricated by applying post-deposition chemical treatment using vaporized ammonia. The calcined samples showed well-ordered hexagonal mesoporous structures. However, titania

matrices appeared to be amorphous. Mesoporous structures were thermally stable up to 500 °C. Mesoporous titania films showed better photo-catalytic activity than anatase nanocrystalline titania films.

Acknowledgements The authors would like to thank BASF (Mt. Olive, NJ) for providing the Pluronic polymers.

References

1. Kresge CT, Leonowicz ME, Roth WJ, Vartuli JC, Beck JS (1992) Nature 359:710-712
2. Beck JA, Vartuli JC, Roth WJ, Leonowicz ME., Kresge CT, Schmitt KD (1992) J Am Chem Soc 114:10834-10843
3. Huo Q, Margolese DI, Ciesla U, Demuth DG, Feng P, Gier TE, Sieger P, Firouzi A, Chmelka BF, Schuth F, Stucky GD (1994) Chem Mater 6:1176-1192
4. Raman NK, Anderson MT, Brinker CJ (1996) Chem Mater 8:682-1701
5. Putnam RL, Nakagawa N, Mcgrath KM, Yao N, Aksay LA, Gruner SM, Navrotsky A (1997) Chem Mater 9:2690-2693
6. Antonelli DM, Ying JY (1996) Chem Mater 8:874-881
7. Antonelli DM, Nakahira A, Ying JY (1996) Inorg Chem 35:3126-3136
8. Chen F, Liu M (1999) Chem Commun 1829-1830
9. Lu Y, Ganguli R, Drewien CA, Anderson MT, Brinker CJ, Gong W, Guo Y, Soyez H, Dunn B, Huang MH, Zink JI (1997) Nature 389:364-368
10. Zhao D, Yang P, Melosh N, Feng J, Chmelka BF, Stucky GD (1998) Adv Mater 10:1380-1385
11. Brinker CJ, Lu Y, Sellinger A, Fan H (1999) Adv Mater 11:579-585
12. Brinker CJ (2004) MRS Bull 29:631-640
13. Grosso D, Soler-illia GJAA, Babonneau F, Sanchez C, Albouy PA, Brunet-bruneau A, Balkenende AR (2001) Adv Mater 13:1085-1090
14. Paik JA, Fan SK, Kim CJ, Wu MC, Dunn B (2002) J Mater Res 17:2121-2129
15. Lundberg M, Skarman B, Cesar F, Wallenberg LR (2002) Microporous Mesoporous Mater 54:97-103
16. Fujishima A, Honda K (1972) Nature 238:37-38
17. Yasumori A, Ishizu K, Hayashi S, Okada K (1998) J Mater Chem 8:2521-2524
18. Mori R, Takahashi M, Yoko T (2005) J Mater Res 20:121-127
19. Forster S, Antonietti M (1999) Adv Mater 10:195-217
20. Yang P, Zhao D, Mragolese DI, Chmelka BF, Stucky GD (1999) Chem Mater 11:2813-2826
21. Antonelli DM (1999) Microporous Mesoporous Mater 30:315-319
22. Wang Y, Tang X, Yin L, Huang W, Hacohen YR, Gedanken (2000) A Adv Mater 12:1183-1186
23. Kitazawa N, Sakaguchi K, Aono M, Watanabe Y (2003) J Mater Sci 38:3069-3072
24. Grosso D, Soler-illia GJ, Crepaldi E, Cagnol F, Sinturel C, Bourgeois A, Brunet-bruneau A, Amenitsch H, Albouy PA, Sanchez C (2003) Chem Mater 15:4562-4570
25. Crepaldi EL, Soler-illia GJ, Grosso D, Ribot F, Sanchez C (2003) J Am Chem Soc 125:9770-9786
26. Smarsly B, Grosso D, Brezesinski T, Pinna N, Boissiere C, Antonietti M, Sanchez C (2004) Chem Mater 16:2948-2952
27. Livage J, Sanchez C, Babonneau F (1998) In: Interrante LV, Hampden-Smith MJ (eds) Chemistry of Advanced Materials: An Overview. Chapter 9. Wiley-VCH, New York
28. Livage J, Henry M, Sanchez C (1988) Progress is Solid State Chem 18:259-341
29. Sanchez C, Livarge J, Henry M, Babonneau F (1988) J Non-Cryst Solids 100:65-76
30. Yin JS, Wang ZL (1999) Adv Mater 11:469-472
31. Zana R (1997) Colloids Surf 123/124:27-35
32. Zhao D, Feng J, Huo Q, Melosh N, Fredrickson GH, Chmelka BF, Stucky GD (1998) Science 279:548-552
33. Zhao D, Huo Q, Feng J, Chmelka BF, Stucky GD (1998) J Am Chem Soc 120:6024-6036